

RSC Advances



This is an *Accepted Manuscript*, which has been through the Royal Society of Chemistry peer review process and has been accepted for publication.

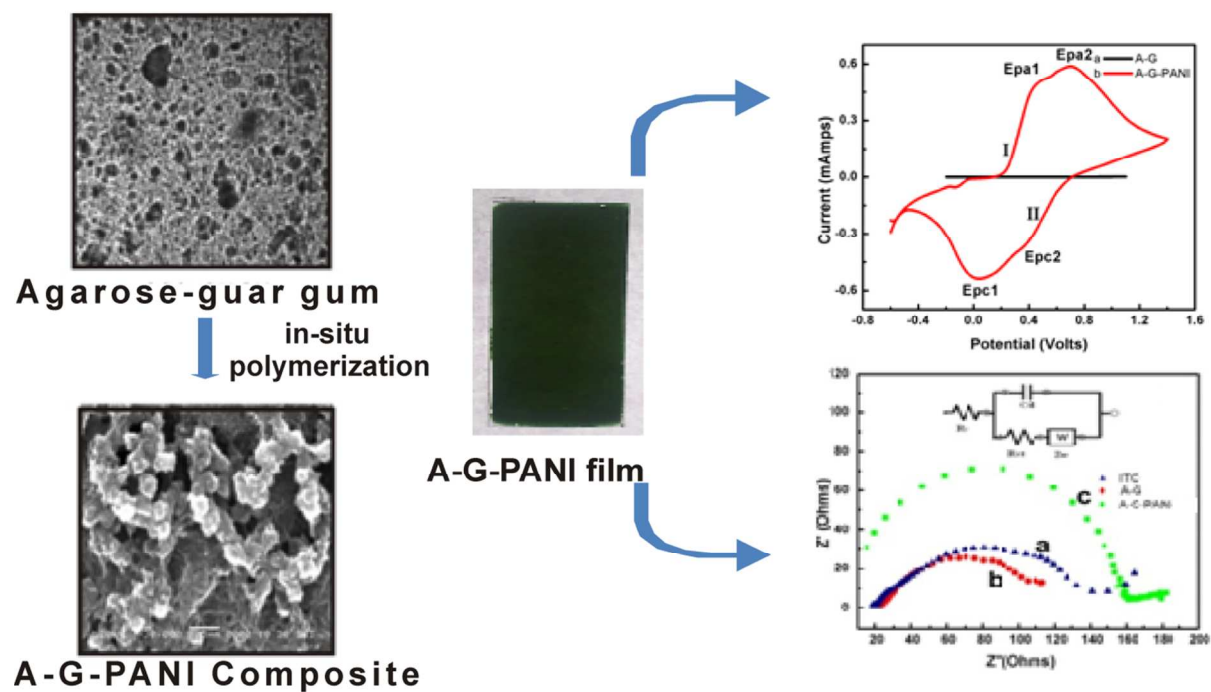
Accepted Manuscripts are published online shortly after acceptance, before technical editing, formatting and proof reading. Using this free service, authors can make their results available to the community, in citable form, before we publish the edited article. This *Accepted Manuscript* will be replaced by the edited, formatted and paginated article as soon as this is available.

You can find more information about *Accepted Manuscripts* in the [Information for Authors](#).

Please note that technical editing may introduce minor changes to the text and/or graphics, which may alter content. The journal's standard [Terms & Conditions](#) and the [Ethical guidelines](#) still apply. In no event shall the Royal Society of Chemistry be held responsible for any errors or omissions in this *Accepted Manuscript* or any consequences arising from the use of any information it contains.

A table of contents entry

An electroactive, electroconducting, processable polyaniline composite is developed via agarose-guar gum assisted polymerization.



Agarose-guar gum assisted synthesis of processable polyaniline composite: morphology and electro-responsive characteristics†

Chetana Vaghela^a, Mohan Kulkarni^{a*}, Meena Karve^{b*}, Rohini Aiyer^c, Santosh Haram^a

a Department of Chemistry, Ganeshkhind Road, Savitribai Phule Pune University, Pune-411007, India.

b Institute of Bioinformatics and Biotechnology, Ganeshkhind Road, Savitribai Phule Pune University, Pune-411007, India.

c Center for Sensor Studies, Department of Electronic Science, Savitribai Phule Pune University, Pune-411007, India

To whom correspondence should be addressed:

Email: meenaskarve@gmail.com, drmvkulkarni@gmail.com

Phone: +91-020- 25696061, +91-020-25691333, Fax: 91-020-25691728

Abstract

The present communication reports, the development of processable polyaniline(PANI) in the film form via agarose-guar gum(A-G) assisted in-situ polymerization of aniline using potassium dichromate as an oxidant. The network structure of A-G not only provides the mechanical support to polyaniline, but also a microporous template, which allows the reinforcement of PANI into nanostructures with interpenetrated polymer network between PANI and A-G, as evidenced by optical microscopy and SEM. The FTIR and TGA analysis confirms the formation of agarose-guar gum-polyaniline composite (A-G-PANI) having hydrogen bonding interactions. A-G-PANI film has better adherence property on the glass substrate as compared with PANI. The A-G-PANI composite shows appreciable DC conductivity in the range of 10^{-3} - 10^{-2} S/cm and electrochemical activity, having oxidation-reduction transitions corresponding to polyaniline. It exhibits both ionic and electronic conductivity as confirmed by EIS. The electro-responsive characteristics exhibited by the novel A-G-PANI composite makes it a promising electrode material for the construction of chemical sensors and biosensors.

Key words: Agarose-guar gum-polyaniline composite, biopolymer assisted synthesis, processable polyaniline, interpenetrated polymer network, electro-responsive.

† Electronic supplementary information (ESI) available: Effect of varying (a)aniline:oxidant molar ratio (b)HCl concentration on the conductivity of A-G-PANI films, UV-Visible spectra of (a)A-G film and (b)A-G-PANI composite film in DMSO, Photographs showing an adhesion test using scotch tape pressed on the surface of (a)A-G-PANI composite films with different PANI content (b)PANI and A-G-PANI composite film, deposited on glass slide, Cyclic voltammogram of polyaniline in 1M HCl at the scan rate of 20 mV/Sec, Comparison of the standard cathodic peak potentials and anodic peak potentials of PANI powder and A-G-PANI film, The values of each component in the Randle equivalent circuit for each electrode/material/electrolyte system.

Introduction

In the recent years, the formation of composite between polyaniline (PANI) and other conventional polymers, which are having good mechanical properties, is gaining much importance. This is in order to overcome the poor processability of PANI, which arises due to infusibility and poor solubility in many solvents.¹ Composite of polyaniline with various organic polymers like polyacrylamide, nylon, nafion, polyvinylalcohol, polystyrene and polyurethane has been previously reported.² Biopolymers like cellulose and its derivatives, chitosan, starch, lignosulfate and acacia gum have also been utilized for the composite formation.³⁻⁷ Biopolymers are preferred choice for this purpose because of cost effective, ecofriendly and biocompatible nature.

Agarose (A) is a biopolymer consisting of alternating β -D-galactopyranose (1-3linked) and 3,6 anhydro- α -L-galactopyranose (1-4 linked) units, forming thermoreversible hydrogel with 3-D network structure. The network structure of agarose is particularly important in various biological and biomedical applications. Guar gum (G) is a galactomannan which acts as a thickening agent, swells in cold water, but does not form aggregates or network structure. Studies have been conducted for the formation of agarose and guar gum composite gel (A-G) and advantages of the interaction between them.^{8,9} Such combination of biopolymers has unique properties, like an excellent membrane forming ability, high permeability towards water, good adhesion, biocompatibility, nontoxicity, high mechanical strength and ability to form a water insoluble microporous structure. This suggests that, such biopolymer composite gel can serve as a potential material for the synthesis of processable polyaniline in the film form. Agarose-guar gum composite gel membrane has been successfully used by our group for enzyme immobilization, which was suitable for construction of various biosensors.^{10,11} With this background, we planned for synthesizing composite of these natural biopolymers with conducting polyaniline, thus imparting novel features to the biopolymer. This kind of approach will widen the scope of biopolymer for various applications.

Interestingly, it has been observed that templated-synthesis of PANI was generally undertaken in achieving the control over the shape and size in nanometer range and to obtain unique morphologies.^{1,12,13} Biopolymer based templated-synthesis of polyaniline is still unnoticed and only a few reports are available. Formation of controlled size polyaniline using crosslinked carboxymethyl chitin, as a biopolymer template has been reported.¹⁴ Agar gel template was also used for the preparation of compact polyaniline film, where polyaniline was electrochemically synthesized.¹⁵

To the best of our knowledge, this is for the first time, agarose-guar gum biopolymer is being used for polyaniline composite formation. The main focus is on the use of the 3-D network structure of agarose-guar gum, which will not only provide mechanical support, but also a microporous template for the synthesis of polyaniline. The

influence of reaction conditions on synthesis of composite and electrical conductivity of A-G-PANI films as a function of these conditions were investigated. The surface morphology of composite and interaction between biopolymer and polyaniline was studied. Further, the electrical and electrochemical analysis of the composite was carried out to study the electro-responsive characteristics.

Experimental

Materials

Analytical grade agarose having medium EEO (Sigma Aldrich), guar gum (SRL-India), analytical grade hydrochloric acid (35%) and potassium dichromate were used as procured. Aniline (AR grade) was double distilled prior to use. The aniline monomer solution was prepared in hydrochloric acid and potassium dichromate solution was prepared in distilled water. Microscopic glass slides were used as substrates to give an additional mechanical support for the deposition. The glass substrates were cleaned by sequentially washing with chromic acid and 10% NaOH solution. In this process, glass slides were kept in the chromic acid solution and heated in a water bath at 70 °C for 10 min, followed by rinsing with distilled water several times. The similar procedure was repeated with 10% NaOH washing. Cleaned slides were air dried in an oven and stored under dust free conditions.

Preparation of agarose-guar gum matrix

Measured amount of agarose powder was added to distilled water and stirred to get uniform suspension of 2% (W/V). It was heated up to 80 °C in water bath to obtain a transparent solution, which ensure complete dissolution of agarose. Guar gum powder was gently dissolved in distilled water without formation of clumps to get 1% (W/V) solution at room temperature ($25 \pm 2^\circ\text{C}$).

Agarose and guar gum solutions were mixed carefully with 1:1(V:V) proportion in order to avoid the formation of air bubbles. The solution of A-G (100 μl , total polymer concentration of 1.5%) was drop cast on a glass slide (1cm^2) to obtain uniform film. On similar lines, only agarose films (1.5% W/V) were also deposited on the glass substrate. The cast films were dried in a hot air oven at 45-50 °C and stored in an airtight container at room temperature to maintain a dust and moisture free environment. This agarose-guar gum biopolymer matrix has been used as a template for the synthesis of conducting polymer. The thickness of A-G film deposited on a glass slide of 1cm^2 was found to be uniform and in the range of $17 \pm 2 \mu\text{m}$, as measured with KLA-Tencor Profilometer (P-16⁺). Similarly, the A-G films having thickness of $47 \pm 3 \mu\text{m}$ were deposited by drop casting 2ml of A-G solution on a glass slide of $7.5 \times 2.5 \text{cm}^2$.

Synthesis of agarose-guar gum-polyaniline (A-G-PANI) composite

Synthesis of polyaniline was carried out using the template of A-G biopolymer matrix prepared as above. These A-G films (total polymer concentration of 1.5%) were kept in aniline monomer solution (0.05M-0.6M), prepared in 1M HCl for 1 hour to achieve maximum swelling of biopolymer, which was checked by weighing the films. The polymerization reaction was initiated by adding the potassium dichromate solution with a concentration equivalent to a molar ratio of 5:1 (aniline:oxidant). The polymerization was carried out for about one hour at a temperature of 24 ± 2 °C. The completion of polymerization was ensured by conductivity measurement (till to get no significant increase in conductivity). After completion of the polymerization, A-G-PANI films were washed with 1M HCl, followed by distilled water to remove unreacted aniline and water soluble products respectively. Aniline monomer concentration was varied in the range of 0.05M to 0.6M, as to achieve different polyaniline content in the composite. The polyaniline content in the composite was determined gravimetrically using the equation: $\text{PANI}(\text{weight}\%) = \frac{W_c - W_b}{W_c} \times 100$, where W_c and W_b are the dry weights of A-G-PANI composite and biopolymer (A-G) respectively. The influence of reaction conditions on electrical conductivity of the films was determined, using four probe method. Polyaniline in the powder form was also synthesized under identical reaction conditions by adopting the previously reported method.¹⁶ Further, the films were deposited on precleaned glass substrate by drop casting the suspension of polyaniline in 1M HCl.

Characterization

The electrical conductivity was measured by four probe method (Jaldel-RM-3), at room temperature (25 ± 2 °C) and at 40% humidity. Four probe method gives sheet resistivity ($R_s, \Omega/$) and by measuring the thickness of the film ($t, \text{cm.}$), Specific resistivity ($\rho = R_s \times t$) and corresponding conductivity ($\sigma = 1/\rho$) of the films were calculated.

UV-visible spectra of A-G-PANI composite in DMSO was recorded by spectrophotometer (Shimadzu UV-C5300). The FTIR spectra of the films were obtained using Bruker Tensor 37 FTIR spectrophotometer, with platinum ATR, considering air as a baseline.

The surface morphology of films was studied by optical microscopy and SEM (Jeol-JSM 6360A). Samples were coated with platinum before imaging and accelerating voltage of 20 Kv was applied to facilitate the imaging. Optical microscopic images of films were taken by using Carl ZIESS Microscope equipped with a primostar digital camera (5 MP), at a total magnification of 100X. Images were processed by TS view software, using the standard calibration scale for the determination of pore size.

Thermogravimetric analysis was performed using a TG analytical system (Shimadzu-DTG-60H) in the temperature range of 25 °C to 900 °C under nitrogen gas atmosphere.

Some of the physical properties of the films were analyzed by the following techniques. The swelling behavior of A-G and A-G-PANI films was studied by gravimetric analysis at room temperature (25 ± 2 °C), in distilled water for 1 hour. The swollen films were removed from distilled water and immediately weighed with microbalance (Citizen-CY 54), after the removal of unabsorbed water from the surface. The swelling ratio was calculated by the equation $(W_{\text{swollen film}} - W_{\text{dried film}}) / W_{\text{dried film}}$, in which W is the weight of films in the swollen and dried form. Relative adherence of A-G-PANI films was ensured with the simple scotch tape press test. In this test, scotch tape (1 cm^2) was pressed firmly on the surface of the glass substrate, where the film is deposited and later on the tape was stripped off the surface. Thus, the relative adherence of the A-G-PANI composite film and only PANI film, deposited on glass substrate was examined. The mechanical properties, including tensile strength, Young's modulus and strain at break of A-G and A-G-PANI composite films were determined by tensile test using a universal testing machine (Llyod instruments-LR 10K plus), with test speed of 0.5mm/min and load cell of 100N. Sample size of 40 mm length, 10 mm width and thickness of $47 \mu\text{m}$ were used. Three specimens were used for each sample in the tensile test.

Electro-responsive characteristics of A-G-PANI films were determined by I-V, cyclic voltametry (CV) and electrochemical impedance spectroscopy (EIS). For I-V measurement, the electrical contacts were made with room temperature curable silver paste. For the CV and EIS, films were deposited on precleaned ITO glass slides with working window of $0.5 \times 0.5 \text{ cm}^2$. I-V and CV were recorded using Autolab potentiostat (3023). An EIS was taken with a Biologic galvanostat /potentiostat in the frequency range of 1 mHZ to 7 MHZ, at the equivalent potential of 35mV. An EIS was recorded with three electrode system in solution of $\text{Fe}(\text{CN})_6^{4-/3-}$ (10mM in 1M HCl). Curve fitting was done by EC Lab software(10.21) using an appropriate Randel equivalent circuit.

Results and discussion

Synthesis of A-G-PANI composite

The scheme for the formation of A-G-PANI composite via biopolymer assisted in-situ polymerization of aniline is described in the Fig. 1a. Agarose-guar gum forms a hydrogel with 3-D network structure, which facilitates the absorption of aniline monomer during the swelling period.^{17,8,9} The agarose-guar gum has a large amount of free hydroxyl group, which helps in the interaction with aniline monomer via hydrogen bonding, that can lead to the uniform distribution of monomer in the network of biopolymer.³ With the subsequent addition of an oxidant, aniline present in the agarose-guar gum matrix undergoes oxidative polymerization and forms polyaniline. The formation of polyaniline in the matrix of agarose-guar gum is demonstrated by the development of dark green coloration of films, with different intensities depending upon the amount of polyaniline in the composite as compared with only A-G film (Fig. 1b).

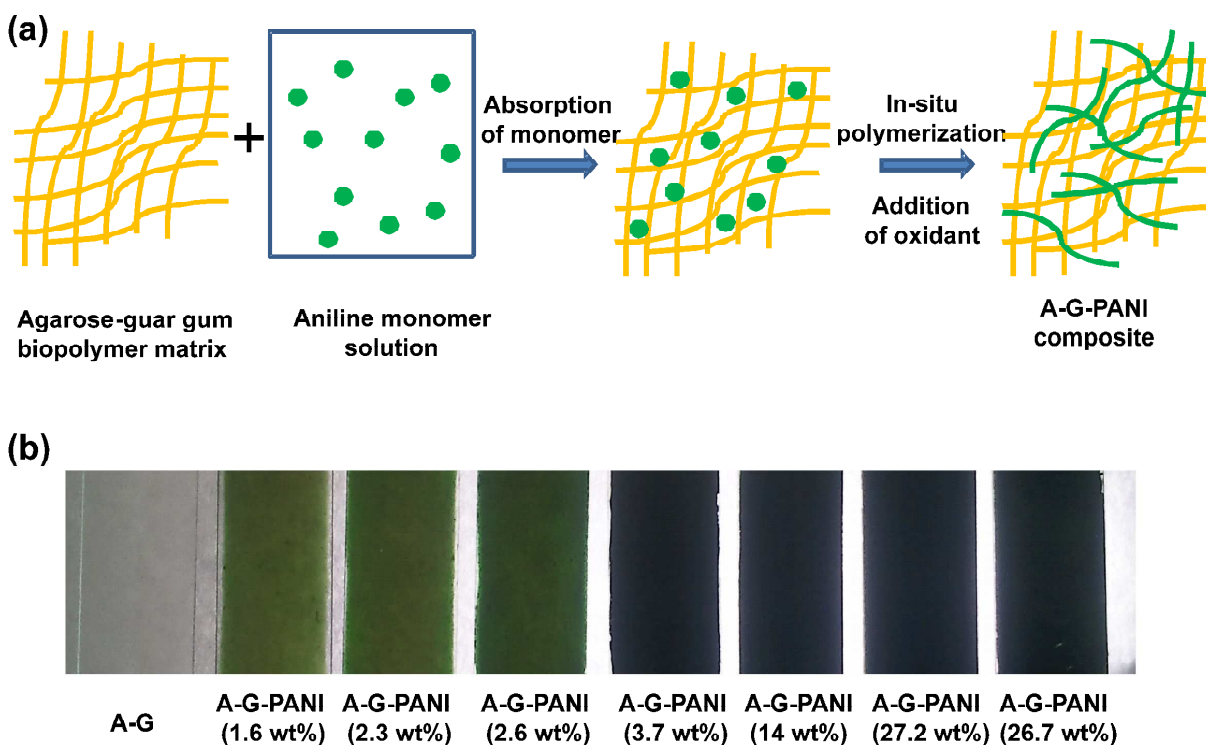


Fig 1. (a) Schematic showing formation of A-G-PANI composite via biopolymer assisted in-situ polymerization of aniline monomer. (b) Photographs of A-G and A-G-PANI composite with different PANI content.

The weight% of polyaniline in A-G-PANI composite synthesized at various concentrations of aniline monomer is given in Table 1. The polyaniline content of 1.6 wt% to a maximum of 27.2 wt% was achieved, by increasing concentration of aniline monomer from 0.05M to 0.5M. Thus, the content of polyaniline in A-G-PANI composite is modulated by varying the concentration of aniline monomer. The higher content of PANI was not observed here for A-G-PANI composite, as agarose-guar gum hydrogel remains attached to the glass substrate, which tends to limit the swelling of hydrogel.¹⁸ The free standing membrane of A-G when used as matrix for in-situ polymerization of aniline, the maximum polyaniline content was observed to be 90%. It is worth to mention here, the film of hydrogen supported on the solid surface is of great importance, as it represents a ‘smart’ coating that can be microstructured and integrated into microfabrication process, especially in the field of biosensors.¹⁸

Table 1. PANI content and electrical conductivity of A-G-PANI composite films as a function of aniline monomer concentration

Samples*	Agarose-guar gum Concentration (%)	Aniline monomer Concentration (M)	PANI (wt%)	Electrical Conductivity (S/cm)
A-G [#]	1.5	-	-	$2.5 \pm 2 \times 10^{-9}$
A-G-PANI-C1	1.5	0.05	1.6%	$4.1 \pm 2 \times 10^{-6}$
A-G-PANI-C2	1.5	0.1	2.3%	$2.3 \pm 1.5 \times 10^{-4}$
A-G-PANI-C3	1.5	0.2	2.6%	$2.9 \pm 1.3 \times 10^{-3}$
A-G-PANI-C4	1.5	0.3	3.7%	$1.3 \pm 2 \times 10^{-2}$
A-G-PANI-C5	1.5	0.4	14%	$3.4 \pm 1 \times 10^{-2}$
A-G-PANI-C6	1.5	0.5	27.2%	$5.4 \pm 1.2 \times 10^{-2}$
A-G-PANI-C7	1.5	0.6	26.7%	$3.1 \pm 1.5 \times 10^{-2}$

* C represents A-G-PANI composite.

[#] Conductivity of A-G film was measured Keithely electrometer-6517 B

Electrical conductivity of A-G-PANI composite

The electrical conductivity of composite films as a function of aniline monomer concentration is shown in Table 1. As demonstrated, aniline monomer concentration is determining the polyaniline content in composite, thus electrical conductivity of A-G-PANI films. The conductivity of A-G-PANI composite films vary by four orders of magnitude in the range of 10^{-6} to 10^{-2} S/cm with different polyaniline content. The A-G-PANI composite with a PANI content of 1.6 wt% and 2.6 wt% exhibits the conductivity in the order of 10^{-6} and 10^{-3} S/cm respectively. The maximum conductivity of $5.4 \pm 1.2 \times 10^{-2}$ S/cm was obtained with the PANI content of 27.2 wt%. The increase in the conductivity of A-G-PANI composite as a function of PANI wt% can be explained on the basis of effective medium theory (Springett model).^{19,20} The conductivity value of developed A-G-PANI composite is more or less comparable with previously reported biopolymer-polyaniline composites. The conductivity of PANI/chitosan and substituted PANI/chitosan composites were found to be in the range of 7.73×10^{-5} , 1.68×10^{-4} , 6.84×10^{-6} and 1.53×10^{-4} S/cm.²¹ Similarly, the conductivity of PANI/rice straw fiber composites with different polyaniline loading were in the range of 1.56×10^{-10} (2.5 wt% PANI), 4.56×10^{-7} (5 wt% PANI), 2.5×10^{-5} (10 wt% PANI) S/cm and conductivity in the order of 10^{-3} S/cm for PANI/lignosulfate composites was observed by other workers.^{22,6} The conductivity of cellulose-PANI blend was reported to be 2.43×10^{-4} (4 wt% PANI), 1.84×10^{-3} (7.8 wt % PANI), 2.71×10^{-3} (9.6 wt% PANI) and 3.0×10^{-2} (21.2 wt% PANI) S/cm.⁴

The electrical conductivity of A-G-PANI films was also found to be influenced by aniline to oxidant molar ratio and HCl concentration, which tends to affect the polymerization process of polyaniline. The aniline to potassium

dichromate ratio of 5 and 1M HCl concentration was optimized to have highest conductivity of A-G-PANI composite (see ESI† Fig. S1).

UV-visible spectral analysis

A-G films did not exhibit any absorption peaks in the UV-visible range. Whereas, UV-visible spectrum of A-G-PANI composite films showed absorption peaks at 330 and 630nm, corresponding to characteristic peaks of polyaniline (ESI† Fig. S2). Peak at 330nm is assigned to π - π^* transition within benzoid ring and peak at 630nm correspond to π - π^* transition within a quinoid ring of polyaniline.^{23,24} Furthermore, the ratio of intensity at 630nm and 330nm (A_{630}/A_{330}) is related to the oxidation state of polyaniline.²⁵ In the present study, this ratio for A-G-PANI composite was found to be 0.5, thereby suggesting an emeraldine state of polyaniline.

FTIR spectra

FTIR analysis was carried out to confirm polyaniline in the A-G-PANI composite and to determine the change in the molecular structure of agarose-guar gum biopolymer, after in-situ synthesis of polyaniline. FTIR spectrum of A-G film showed bands, corresponding to characteristic bands of agarose and guar gum (Fig. 2a). The band at 929cm^{-1} can be assigned to the stretching vibration of the C-O-C bridge of 3,6-anhydro-L-galactopyrose in agarose and the band at 1034cm^{-1} is due to glycosidic bond stretching in agarose and guar gum. While the band at 1640cm^{-1} correspond to C=O stretching vibration, characteristic of the saccharide structure and the band at 3307cm^{-1} is related to -OH stretching in agarose and guar gum.^{26,27}

A-G-PANI composite film showed the FTIR spectrum resembling to the A-G biopolymer (Fig. 2b). For A-G-PANI composite film, the bands are observed at 929cm^{-1} , 1035cm^{-1} , 1637cm^{-1} , 3222cm^{-1} corresponding to the agarose-guar gum along with the appearance of new bands at 1235cm^{-1} , 1300cm^{-1} , 1491cm^{-1} , 1577cm^{-1} . These bands correspond to characteristic bands of polyaniline (fig. 2c), thereby confirming the development of A-G-PANI composite. Bands at 1491cm^{-1} and 1577cm^{-1} belongs to the C=C stretching vibration in benzoid and quinoid ring in polyaniline, while bands at 1300cm^{-1} and 1235cm^{-1} are due to C-N stretching of the quinoid and benzoid ring in polyaniline.²⁸

Moreover, the broadening of -OH band in the region of $3000\text{-}3700\text{cm}^{-1}$ for A-G-PANI composite as compared with A-G biopolymer, indicate the formation of hydrogen bonding between amino N-H of polyaniline and -OH group of the agarose-guar gum biopolymer. Such interaction was previously reported between polyaniline and other polymers such as nanofibrillated cellulose, polyacrylonitrile, chitosan, poly (N-vinyl-2-pyrrolidone).^{3,21,29,30} In the case of substituted polyaniline/chitosan composites broadening of band between $2878\text{-}3435\text{cm}^{-1}$ was reported due to hydrogen-oxygen interaction between N-H and -OH groups of PANI and chitosan respectively.²¹

Similarly, the decrease in the peak intensity characteristic of –OH bands of iota-carrageenan in the region 2500–3500 cm^{-1} was reported due to hydrogen bonding interaction between –OH and N-H groups of iota-carrageenan and PANI in the composite.³¹ The weakening of OH peak at around 3400 cm^{-1} in nanofibrillated cellulose-polyaniline composite as compared to only nanofibrillated cellulose has been ascribed for hydrogen bonding interaction between them.³

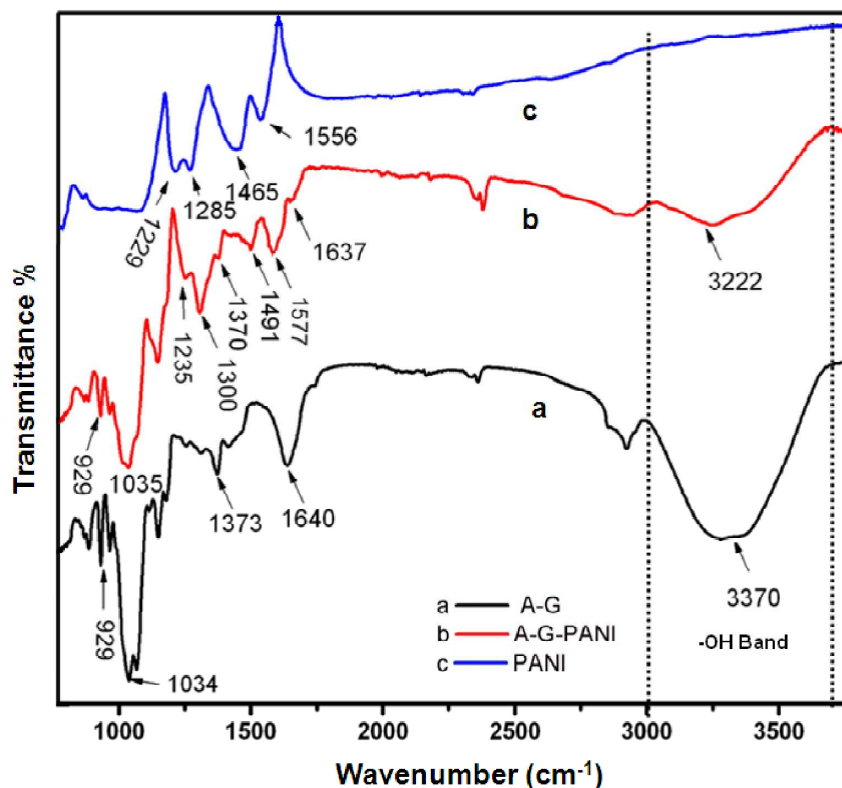


Fig. 2. FTIR spectra of (a) A-G film (b) A-G-PANI composite and (c) PANI powder.

Morphology of A-G-PANI composite: Optical microscopy and SEM analysis

Optical images of agarose-guar gum film and only agarose film showed the distinct morphological differences between them. An extended network (Fig. 3b) is observed for A-G film as compared with the compact network of agarose (Fig. 3a). The A-G film has larger pore size and wider pore size distribution (Fig. 3d) as compared with agarose film (Fig. 3c). The pore size of A-G film is found to be in the range of $13.5 \pm 6 \mu\text{m}$ hence, it can offer a template for the growth of polyaniline.

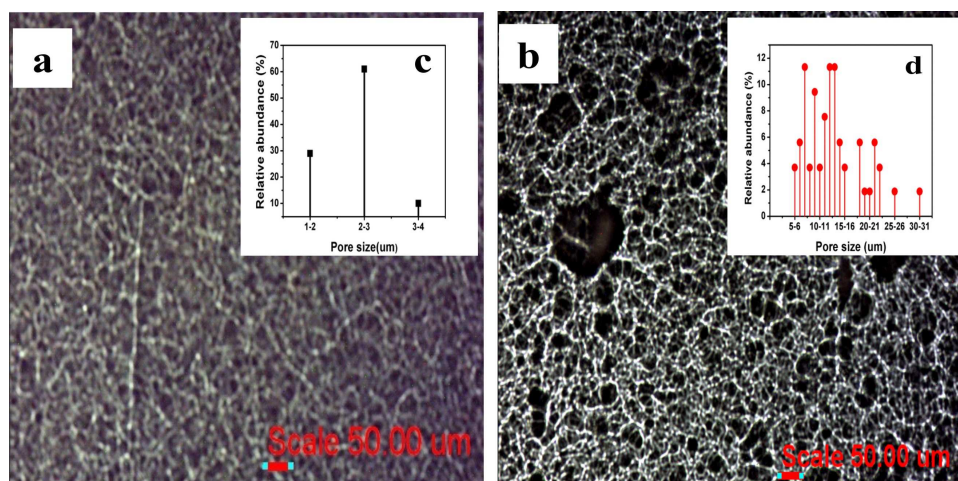


Fig. 3. Optical image of (a) Agarose film (1.5%) (b) A-G film (total polymer concentration 1.5%) at 100X magnification. (c) & (d) indicate the pore size (μm) distribution of agarose and A-G films.

SEM images revealed an uneven surface for the A-G film (Fig. 4a), while agglomerated polyaniline particles with spherical morphology ($0.4 \pm 0.1 \mu\text{m}$) was observed for PANI powder (Fig. 4b). SEM image of A-G-PANI composite indicated the growth of nanostructured polyaniline inside the pores of A-G film, with particle size in the range of $70 \pm 20 \text{ nm}$ (Fig. 4c & 4d). It also showed the linkages between these polyaniline particles, which resembles as a network of polyaniline (Fig. 4c & 4d). Based on optical microscopy and SEM analysis, formation of an interpenetrated network between agarose-guar gum and PANI can be proposed. A similar morphology was observed for poly(acrylate-aniline) composite.^{32,33} As observed, the agarose-guar gum being a porous structure, has a strong absorption capacity, which causes the absorption of large amount of aniline monomer in the matrix. On subsequent addition of an oxidant, aniline present in the pores of biopolymer matrix undergoes oxidative polymerization and forms polyaniline. During the process of polymerization, polyaniline may integrate at some point, as the pores of A-G are randomly oriented. This is an interpenetrated network of polymer, in which biopolymer(A-G) is in the form of 3-D network while polyaniline remains in the chain configuration, which is either free or interlinked.³⁴ The large pore size, wide pore size distribution and less cross-linking density of agarose-guar gum film might have played a role in the development of such morphology.

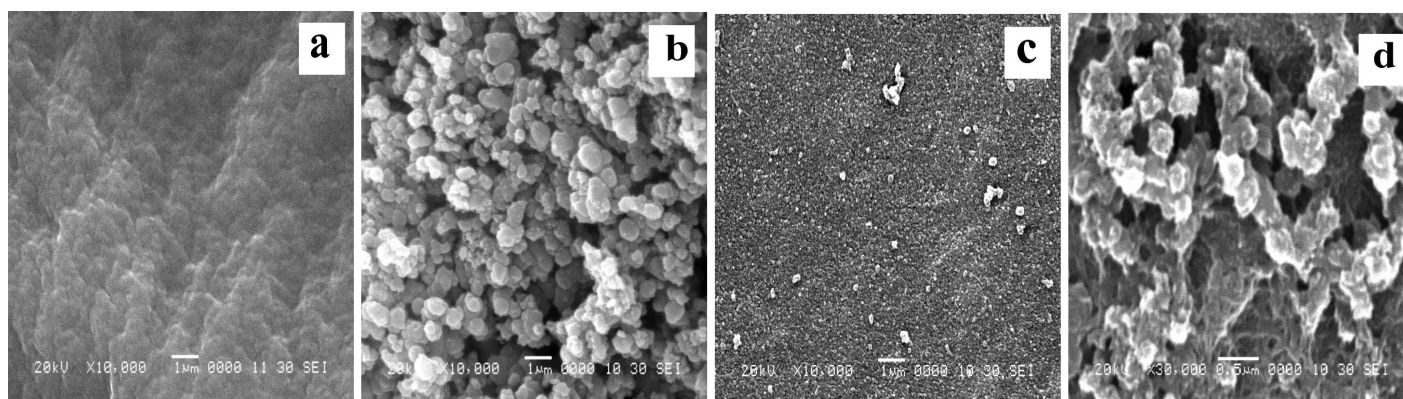


Fig. 4. SEM images of (a) A-G film, (b) PANI powder and (c) and (d) A-G-PANI film at different magnification.

Thermogravimetric analysis

The thermal stability of A-G-PANI composite film (14 wt% PANI) was determined by TGA using PANI and A-G film as a reference. Thermogram of A-G film (Fig. 5a), indicated thermal degradation of this biopolymer in three stages. It showed an initial 31% of weight loss up to 141 °C, due to dehydration, while the rapid decomposition of biopolymer started in the range of 250 °C to 320 °C with the weight loss of 40% and final degradation to constituent elements (C, H, O) occurred at 478 °C.^{35,36} PANI is much more thermally stable, with an initial weight loss of 35% up to 200 °C, due to dopant (Cl) losses (Fig. 5c). Polymer decomposition begins at 360 °C with the residual weight of 52% at 478 °C. The complete degradation of PANI was observed at 940 °C.³⁷ Composite film of A-G-PANI (14 wt% PANI) had thermal degradation intermediate to A-G and polyaniline. It showed only 28% weight loss up to 200 °C, because of moisture and dopant losses, which is much less as compared to constituent polymers. This may be due to the formation of interpenetrated network structure, preventing the loss of small molecules like dopant.³⁷ Composite film had gradual polymer degradation with weight loss of only 12% in the range of 250 °C-320 °C, this weight loss was found to be lower as compared with A-G film. The complete degradation of A-G-PANI composite was achieved at 882 °C (Fig. 5b). The increased thermal stability of A-G-PANI film as compared to A-G film, is due to formation of composite with interpenetrated polymer network. These results are in agreement with previous report indicating the enhanced thermal stability of PANI-chitosan due to composite formation.^{4,38}

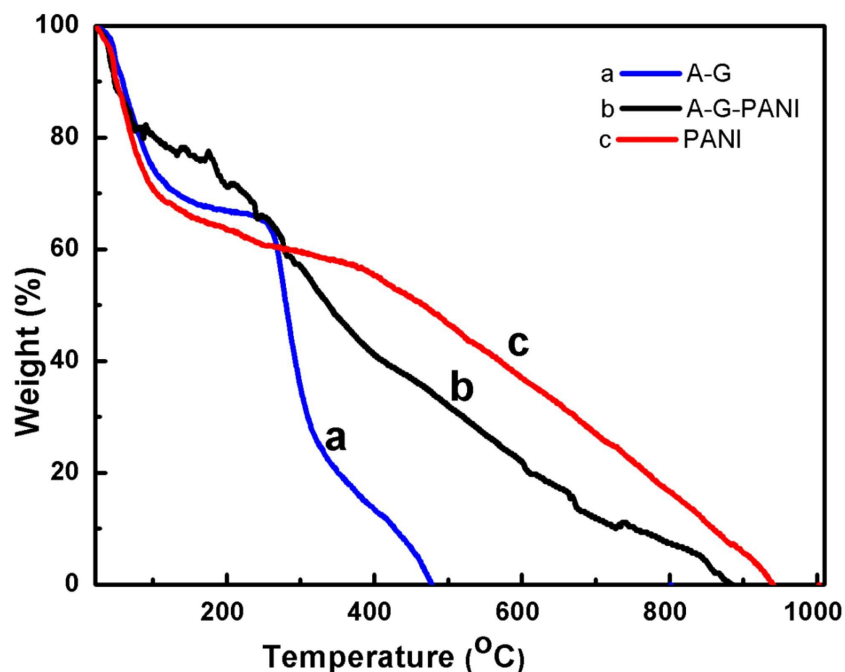


Fig. 5. TGA thermograms of (a) A-G film, (b) A-G-PANI composite film (14 wt% PANI) and (c) PANI powder.

Physical characterization

Swelling study of A-G and A-G-PANI films was carried out to understand the cross linking density of polymeric matrix. The results of the swelling study showed that, swelling ratio of A-G-PANI film (1.7 ± 0.5) was less as compared to A-G film (3.6 ± 0.4), indicating an increased cross-linking density. This is due to the development of interpenetrated network between polyaniline and agarose-guar gum.

The simple scotch tape press test was used to qualitatively estimate the relative adhesiveness of A-G-PANI film and PANI film deposited on a glass substrate.³⁹ It was observed that PANI film was almost detached from the glass surface, while A-G-PANI composite films upto 14 wt% PANI remains firmly attached on the glass substrate, confirming better adhesive property of A-G-PANI composite film (ESI† Fig. S3). The formation of a stable composite film of polyaniline using biopolymer assisted synthesis has demonstrated the processability of polyaniline. Moreover, we have also observed that, A-G-PANI composite films prepared by mixing of polyaniline in molten agarose-guar gum composite gel showed complete loss of film forming ability with different polyaniline content (0.1%, 1%, 5% W/V), thereby indicating the advantage of in-situ polymerization in the biopolymer matrix, which is exploited in the present report for the development of A-G-PANI composite.

The mechanical properties of A-G and A-G-PANI composite films with different polyaniline content are presented in Table 2. Agarose-guar gum film has high tensile strength, Young's modulus and strain at break (26.9 Mpa, 1.0 Gpa and 8.8% respectively). High mechanical properties of A-G biopolymer are due to strong intra- and intermolecular hydrogen bonding formed during the gelation process.⁴⁰ The Young's modulus of the composite films with different PANI content remains more or less same as of A-G film, within the experimental errors. The tensile strength and strain at break are less for A-G-PANI composite films as compared with A-G film, indicating that the A-G-PANI composite films are more brittle than that of pure A-G film. However, tensile strength among A-G-PANI composite with different polyaniline content show some variation. Tensile strength increases with PANI content upto 14wt%, then it decreases. This may be due to more uniform distribution of PANI in biopolymer matrix with increasing PANI content. The similar kind of variation was reported for chitosan/PANI blend, tensile strength decreases initially with the addition of 10% PANI, while it increases further with the addition of 20-40% PANI and again decrease at 50%. The increase in tensile strength was reported due to more uniform distribution of PANI in chitosan matrix.⁴ The strain at break for A-G-PANI composite decreases substantially with increasing PANI content in the composite. Thus, the scotch tape test and tensile test of A-G-PANI composite demonstrated a processability of PANI, by formation of a stable composite film with better mechanical properties. These results suggest that, the processability of polyaniline can be improved by composite development with biopolymer like agarose-guar gum.

Table 2. Mechanical properties of A-G and A-G-PANI composite films.

Samples	Tensile strength (MPa)	Young's modulus (Gpa)	Strain at break (%)
A-G	26.9 \pm 5	1.0 \pm 0.8	8.8 \pm 5
A-G-PANI (1.6 wt%)	5.5 \pm 2	1.0 \pm 0.1	4.7 \pm 0.3
A-G-PANI (2.3 wt%)	7.9 \pm 1.6	1.2 \pm 0.2	2.7 \pm 1.7
A-G-PANI (2.6 wt%)	12.4 \pm 5	1.1 \pm 0.5	1.7 \pm 0.2
A-G-PANI (14 wt%)	22 \pm 6	1.2 \pm 0.4	1.3 \pm 0.1
A-G-PANI (27.2 wt%)	6 \pm 5	1.2 \pm 0.2	1.1 \pm 0.1
PANI	-	-	-

The electro responsive characteristics of A-G-PANI composite were studied by I-V measurements, cyclic voltammetry and electrochemical impedance spectroscopy (Fig. 6, 7 and 8).

Current-voltage relationship (I-V measurements)

According to the I-V plot, current values obtained at any potential for A-G-PANI film (Fig. 6b) were found to be more as compared with A-G film (Fig. 6a), indicating enhanced electrical conductivity of A-G-PANI composite. The electrical conductivity of A-G-PANI film is due to proton hopping along the PANI chains in A-G-PANI composite.⁴¹

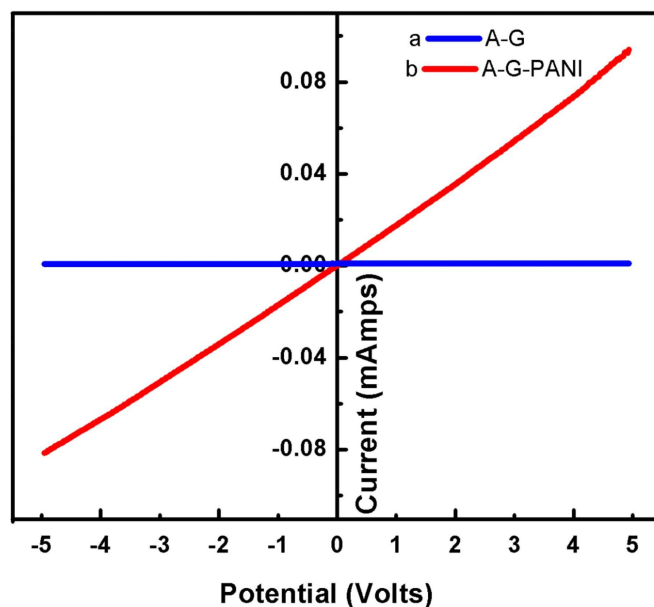


Fig. 6. I-V plot of (a) A-G film (b) A-G-PANI composite film

Cyclic voltammetry analysis

Cyclic voltammogram of A-G film did not show any oxidation or reduction peaks (Fig. 7[I] a), indicating the absence of electrochemical activity. While cyclic voltammogram of A-G-PANI composite film (Fig. 7[I] b) showed reversible redox electrochemical activity having distinct oxidation and reduction peaks corresponding to the transition of polyaniline into its different oxidation states at scan rate of 20mV/Sec. In the voltammogram of A-G-PANI composite during the direct scan (I), Epa1 corresponds to transition from the leucoemeraldine state to the emeraldine state and Epa2, corresponding to the transition from the emeraldine state to the perigranine state. While in the inverse scan (II), reduction process is observed. An Epc2 corresponding the conversion of perigranine to emeraldine state, while emeraldine to leucoemeraldine conversation take place at Epc1.⁴² This

electrochemical behavior observed for composite film of A-G-PANI was similar to the standard electrochemical behavior of polyaniline. The voltammogram and characteristic peak potentials (Epa1&2; Epc1&2) obtained for the composite is slightly different than the standard peak potentials observed for only polyaniline prepared under similar conditions (See ESI† Fig. S4 and Table S1). This behavior can be attributed to composite development and the interaction occurred between polyaniline and agarose guar gum biopolymer.

Moreover, the redox electrochemical activity of A-G-PANI composite film was found to vary with respect to solution pH (Fig. 7[II]). This phenomenon is due to pH dependent transition of emeraldine salt to emeraldine base (Fig. 7[II] inset), thereby leading to different charge density at the interface of A-G-PANI composite and aqueous phase. This pH responsive ability of A-G-PANI composite can be exploited for the development of pH transducer, which is an essential component of many chemical and biochemical sensors.

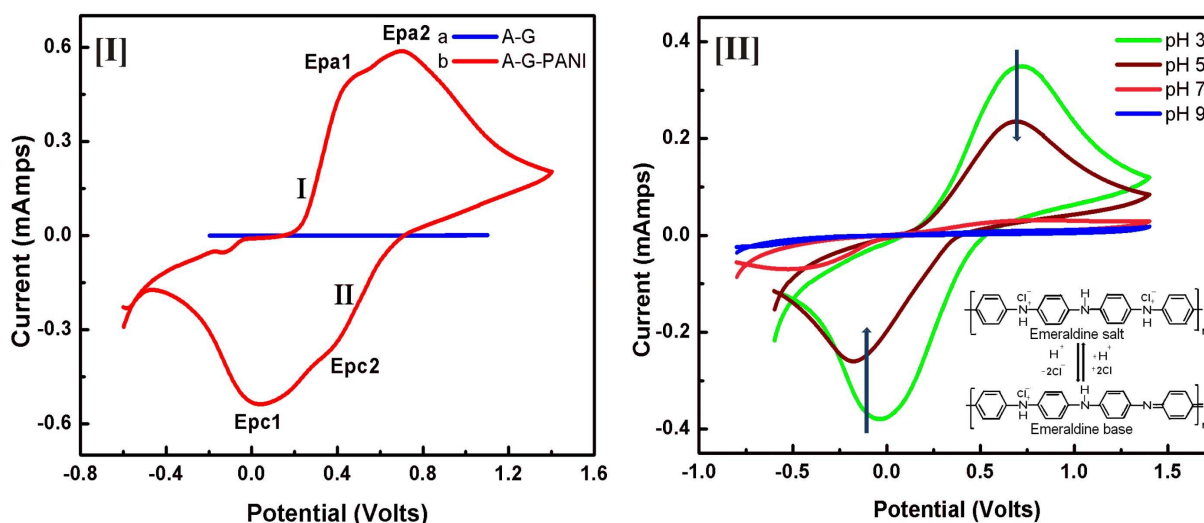


Fig. 7. [I] Cyclic voltammogram of (a) A-G film, (b) A-G-PANI composite film in 1M HCl at the scan rate of 20mV/Sec. [II] Cyclic voltammogram of A-G-PANI composite at different pH and inset is polyaniline conversion from salt to base form.

Electrochemical impedance spectroscopic analysis

Electrochemical impedance spectroscopy is an effective tool to obtain an insight of electrochemical reaction occurring at the surface of the modified electrode. The EIS curve for (a) ITO, (b) ITO/A-G, (c) ITO/A-G-PANI composite film (2.3 wt% PANI) and (d) ITO/A-G-PANI composite film (14 wt% PANI) is shown in Fig. 8 (I) and (II) with the appropriate Randle equivalent circuit. In Randle's circuit, it was assumed that the resistance to charge transfer (R_{ct}) and the Warburg impedance (W) were both in parallel to the double layer capacitance (C_{dl}), this parallel combination of R_{ct} and C_{dl} gives rise to a semicircle in the complex plane plot of imaginary (Z'') against

real(Z') part of impedance.^{43,44} It is well established that the comparison of R_{ct} is an important parameter in stating the effectiveness of the coated electrode material for the charge transfer from the solution to the electrode. It was observed that ITO/A-G modified electrode has lowest R_{ct} value (49.76 ± 0.2 Ohm) due to excellent ionic conduction offered by a three-dimensional network of neutral biopolymer (agarose-guar gum). R_{ct} values were found to be higher for A-G-PANI composite films as compared with A-G film (see ESI† Table S2). Perhaps, this was expected as PANI exhibit capacitive behavior on the surface of the electrode.^{45,46} Higher R_{ct} is observed for composite film with 14 wt% PANI ($R_{ct} = 2.169 \times 10^6 \pm 0.3$ Ohm), as compared with composite film with 2.3 wt% PANI ($R_{ct} = 230.2 \pm 0.1$ Ohm), due to more amount of polyaniline. It should be noted that the excellent ionic conductivity offered by agarose-guar gum film becomes significant in accelerating the charge transfer ability. The similar kind of decreased R_{ct} and accelerated electron transfer was observed with graphene-cadmium sulfate quantum dots-agarose modified electrode.⁴⁷

The Nyquist diagrams of A-G-PANI composite films (Fig. 8) showing a large semicircle in the wider frequency region indicating electronic conductivity of A-G-PANI composite, is due to both ionic and electrical conductions, offered by the combination of ionic conducting biopolymer(A-G) and electrically conducting polymer(polyaniline). These detailed studies on AC and DC conductivity of A-G-PANI composites with different polyaniline content forms the necessary base to modulate the properties of composite according to the requirements during the construction of electrical and electrochemical sensors.

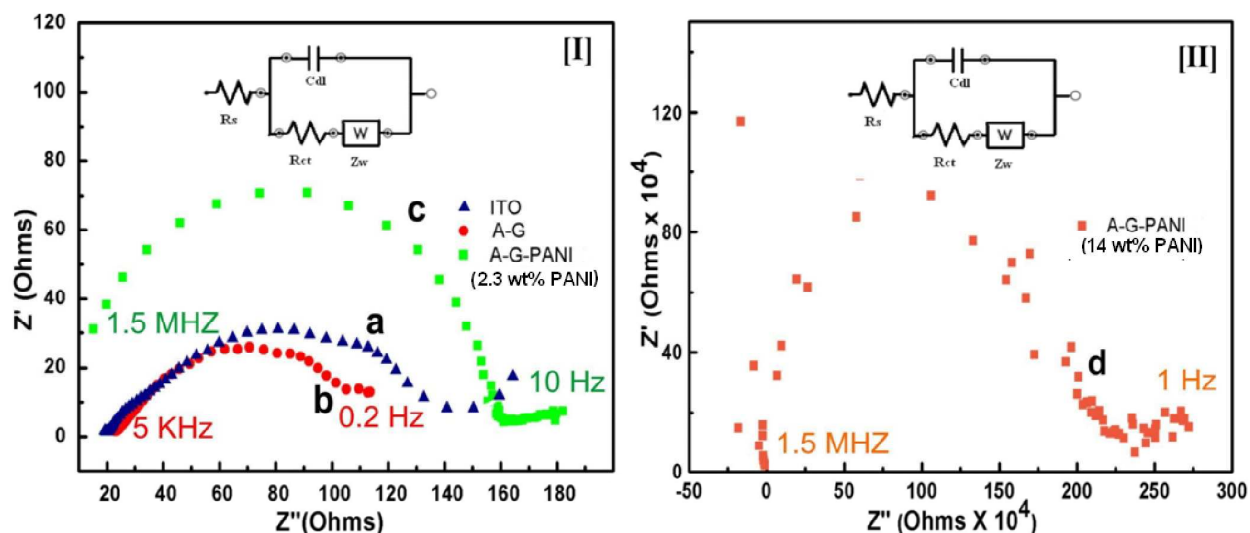


Fig. 8. Nyquist plot of [I] (a) ITO, (b) ITO/A-G and (c) ITO/A-G-PANI with 2.3 wt% PANI [II] (d) ITO/A-G-PANI with 14 wt% PANI. The inset is an equivalent Randle circuit diagram.

Conclusions

A novel composite of agarose-guar gum-polyaniline was successfully prepared via biopolymer assisted synthesis of polyaniline. The incorporation of PANI in A-G film has conferred electrical conductivity, electrochemical activity and enhanced thermal stability to biopolymers, while PANI has acquired improved morphology and processability. A-G-PANI films were characterized by UV-visible, FTIR spectroscopy, SEM and TGA, which confirmed the development of composite with interpenetrated network structure between A-G and PANI. The composite films are electrically conducting (10^{-3} - 10^{-2} S/cm), the electrical conductivity is dependent on polyaniline content in the A-G-PANI composite. I-V, CV and EIS studies have provided insight into electrical and electrochemical behavior of the composite and also demonstrated the processability of A-G-PANI film as a stable electrode material. A-G-PANI films are electrochemically active and having both ionic and electronic conductivity. A-G-PANI composite is exhibiting better mechanical property combined with appreciable electrical properties, which can potentially be used as electrode material in the development of electrochemical sensor and biosensor design.

Acknowledgements

Authors C. Vaghela and M. Karve gratefully acknowledge U.G.C, New Delhi, for the Meritorious Fellowship and Emeritus Fellowship respectively. Authors are thankful to Ganesh Markad, Department of Chemistry, University of Pune, for the help during EIS measurements and Ajinkya Trimukhe And Dr. R. R. Deshmukh, Department of Physics, Institute of Chemical Technology for providing UTM facility.

References

1. Bhadra, S., Khastgir, D., Singha, N. K., Lee, J. H. (2009). *Prog. Polym. Sci.*, 34, 783-810.
2. Anand, J., Palaniappan, S., Sathynarayana, D. N. (1998). *Prog. Polym. Sci.*, 23, 993-1018.
3. Luong, N. D., Korhonen, J. T., Soinen, A. J., Ruokolainen, J., Johansson, L., Seppala, J. (2013). *Eur. Polym. J.*, 49, 335-344.
4. Thanpitcha, T., Sirivat, A., Jamieson, A. M., Rujiravanit, R. (2006). *Carbohydr. Polym.*, 64, 560-568.
5. Janaki, V., Vijayaraghavan, K., Oh, B-T., Lee, K-J., Muthuchelian, K., Ramasamy, A. K., Kamala-Kannan, S. (2012). *Carbohydr. Polym.*, 90, 1437-1444.
6. Roy, S., Fortier, J. M., Nagarajan, R., Tripathy, S., Kumar, J., Samuelson, L. A., Bruno, F. F. (2002). *Biomacromolecules*, 3 (5), 937-941.
7. Tiwari, A., Singh, V. (2008). *Carbohydr. Polym.*, 74, 427-434.
8. Garcia, R. B., Lopes, L., Andrade, C. T. (1992). *Fresenius. J. Anal. Chem.*, 344, 510-513.
9. Garcia, R. B., Andrade, C. T. (1997). *Carbohydr. Polym.* 34, 157-163.

10. Tembe, S., Karve, M., Inamdar, S., Haram, S.K., Melo, J., D'Souza, S. F., (2006). *Anal. Biochem.*, 349, 72-77.
11. Bagal, D. S., Vijayan, A., Aiyer, R.C., Karekar, R.N., Karve, M.S. (2007). *Biosens. Bioelectron.*, 22, 3072–3079.
12. Parthasarathy, R. V., Martin, C. R. (1994). *Chem. Mater.*, 6, 1627-1632.
13. Zhang, D., Wang, Y. (2006). *Mater. Sci. Eng., B*, 134, 9-19.
14. Thanpitcha, T., Sirivat, A., Jamieson, A. M., Rujiravanit, R. (2009). *J. Nanopart. Res.*, 11, 1167-1177.
15. Sung, J., Kim, S., Lee, K. (2004). *J. power sources*, 126, 258-267.
16. Chowdary, P., Shah, B. (2005). *Indian J. Chem. Technol.*, 12, 671-675.
17. Dai, B., Matsukawa S. (2012). *Food Hydrocolloids*, 26, 181-186.
18. Mateescu A., Wang Y., Dostalek J., Jonas U. (2012). *Membranes*, 2, 40-69.
19. Vittal, N., Aiyer, R. C., Aiyer, C. R., Setty, M. S., Phadke, R. N. (1988). *J. Appl. Phys.* 64, 5244
20. Kadam, M.R., Vittal, N., Karekar, R.N., Aiyer, R.C.(1990) *Thin solid films*, 186, 199-208
21. Yavuz, A. G., Uyguna, A., Bhethanabotla, V. R. (2010). *Carbohydr. Polym.*, 81, 712–719.
22. Youssef, A. M., El-Samahy, M. A., & Abdel Rehim, M. H. (2012). *Carbohydr. Polym.*, 89(4), 1027–1032.
23. Cao, Y., Li, S. Z., Xuea, Z. J., Guo, D. (1986). *Synth. Mat.*, 16, 305-315.
24. Libert, J., Cornil, J., Santos, D. A., Bredas, J. L. (1997). *Phys. Rev. B: Condens. Matter Mater. Phys.*, 56, 8638.
25. MacDiarmid, A. G., Epstein, A. J. (1992). *Polyaniline: synthesis, chemistry and processing*, New Aspects of Organic Chemistry II, VCH (Weinheim) and Kodansha (Tokyo) – Copublishers.
26. Pereira, L., Sousa, A., Coelho, H., Amado, A. M., Ribeiro-Claro, P J. A. (2003). *Biomol. Eng.*, 20, 223-228.
27. Wuttisela, K., Panijpan, B., Triampo, W., Triampo, D. (2008). *Polymer (Korea)*, 32, 537-543.
28. Yelil Arasi, A., Juliet Latha Jeyakumari, J., Sundaresan, B., Dhanalakshmi, V., Anbarasan, R. (2009). *Spectrochim. Acta, Part A*, 74 , 229–1234.
29. Pan, W., Yang, S. L., Li, G., Jiang, J. M. (2005)., *Eur. Polym. J.* 41, 2127–2133.
30. Dispenza, C., Lo Presti, C., Belfiore, C., Spadaro, G., Piazza, S. (2006). *Polymer*, 47, 961–971.
31. Vega–Rios, A., Olmedo–Martinez, J., Farias–Mancilla, B., Hernandez–Escobar, C., Zaragoza–Contreras, E. A. (2014)*Carbohydr. Polym.*, 110, 78–86
32. Tang, Q., Lin, J., Wu, J., Zhang, C., Hao, S. (2007). *Carbohydr. Polym.*, 67, 332–336
33. Xia, Y., Zhu, H. (2011). *Soft Matter*, 7, 9388-9393.

34. Klempner, D., Sperling, L. H., Utracki, L. A. (1994). Interpenetrating polymer networks. American Chemical Society publication, Vol. 239.
35. Zohuriaan, M. J., & Shokrolahi, F. (2004). *Polym. Test.*, 23 (5), 575-579.
36. Zhang, L., Wu, C., Huang, J., Peng, X., Chen, P., Tang, S. (2012). *Carbohydr. Polym.*, 88, 1445-1452.
37. Wei, Y., Hsueh, K. F. (1989). *J. Polym. Sci., Part A: Polym. Chem.*, 27 (13), 4351–4363.
38. Jeevananda T., Begum M., Siddaramaiah. (2001). *Eur. Polym. J.*, 37, 1213-1218
39. Mattox, D. M. (1978). Thin film adhesion and adhesive failure-a perspective, adhesion measurement of thin films, thick films, and bulk coatings, ASTM STP 640, K.L. Mittal, Editor, American society for testing and materials, 54.
40. Dai, B., Matsukawa S. (2013). *Carbohydr. Res*, 365, 38-45.
41. Song, E., Choi, J.W. (2013). *Nanomaterials*, 3, 498-523.
42. Pruneanu, S., Veress, E., Marian, I., Oniciu, L. (1999). *J. Mater. Sci.*, 34, 2733– 2739.
43. Barsoukov, E., Macdonald, J. R., (2005). *Impedance Spectroscopy: Theory, Experiment, and Applications* (2nd Ed.). New jersey: John Wiley & Sons, Inc.
44. Lasia, A. (1999). Electrochemical impedance spectroscopy and its applications. *Modern aspects of electrochemistry*, 32, 143-248.
45. Conway, B. E. (1999). *Electrochemical supercapacitors: scientific fundamentals and technological applications*. New York: Kluwer Academic/Plenum Publishers.
46. Hu, C-C., Chu, C-H. (2000). *Mater. Chem. Phys.*, 65
47. Guo, Z., Hao, T., Duan, J., Wang, S., Wei, D. (2012). *Talanta*, 89, 27– 32. .